HHS Public Access

Author manuscript

Matrix Biol. Author manuscript; available in PMC 2016 February 10.

Published in final edited form as:

Matrix Biol. 2014 June ; 36: 64–76. doi:10.1016/j.matbio.2014.04.005.

Matrilysin/Matrix Metalloproteinase-7(MMP7) Cleavage of Perlecan/HSPG2 Creates A Molecular Switch to Alter Prostate Cancer Cell Behavior

B.J. Grindel[1], **J.R. Martinez**[1], **C.L. Pennington**[5], **M. Muldoon**[3,*], **J. Stave**[3], **L.W. Chung**[4], and **M.C. Farach-Carson**[1,2]

[1]Department of Biochemistry and Cell Biology, Rice University, Houston, TX, 77005

[2]Department of Bioengineering, Rice University, Houston, TX 77005

[3]Strategic Diagnostics Inc, Newark DE, 19702

[4]Uro-Oncology Research Program, Samuel Oschin Comprehensive Cancer Institute at Cedars-Sinai Medical Center, Los Angeles, CA, 90048

[5]Shared Equipment Authority, Rice University, Houston, TX 77005

Abstract

Perlecan/HSPG2, a large heparan sulfate (HS) proteoglycan, normally is expressed in the basement membrane (BM) underlying epithelial and endothelial cells. During prostate cancer (PCa) cell invasion, a variety of proteolytic enzymes are expressed that digest BM components including perlecan. An enzyme upregulated in invasive PCa cells, matrilysin/matrix metalloproteinase-7 (MMP-7), was examined as a candidate for perlecan proteolysis both *in silico* and *in vitro*. Purified perlecan showed high sensitivity to MMP-7 digestion even when fully decorated with HS or when presented in native context connected with other BM proteins. In both conditions, MMP-7 produced discrete perlecan fragments corresponding to an origin in immunoglobulin (Ig) repeat region domain IV. While not predicted by *in silico* analysis, MMP-7 cleaved every subpart of recombinantly generated perlecan domain IV. Other enzymes relevant to PCa that were tested had limited ability to cleave perlecan including prostate specific antigen, hepsin, or fibroblast activation protein α. A long C-terminal portion of perlecan domain IV, Dm IV-3, induced a strong clustering phenotype in the metastatic PCa cell lines, PC-3 and C4-2. MMP-7 digestion of Dm IV-3 reverses the clustering effect into one favoring cell dispersion. In a C4-2 Transwell® invasion assay, perlecan-rich human BM extract that was pre-digested with MMP-7 showed loss of barrier function and permitted a greater level of cell penetration than untreated BM extract. We conclude that enzymatic processing of perlecan in the BM or territorial

To whom correspondence should be addressed: Mary C. Farach-Carson, Ph.D., Department of Biochemistry and Cell Biology, Rice University, 6100 Main Street MS140, Houston, TX 77005, USA, Tel.:(713) 348-5052, Fax: (713) 348-5154, farachca@rice.edu.
*Current Address: Romer Labs Technology, Inc. 130 Sandy Drive, Newark, DE 19713, U.S.A.

matrix by MMP-7 as occurs in the invasive tumor microenvironment acts as a molecular switch to alter PCa cell behavior and favor cell dispersion and invasiveness.

Keywords

Perlecan/HSPG2; prostate cancer; matrix metalloproteinase-7/MMP7; matrilysin

1. Introduction

For metastasis and dispersion of cancers originating in epithelial tissues to occur, epithelial cancer cells adopt an invasive mesenchymal-like phenotype that allows them to first remove and then move through the underlying protein-rich basement membrane (BM) and blood vessel rich connective tissue matrix (Polyak and Weinberg, 2009; Rowe and Weiss, 2008). The large heparan sulfate proteoglycan (HSPG) perlecan/HSPG2 is a core component of the BM along with laminin, collagen IV, and nidogen/entactin (Whitelock et al., 2008). For prostate cancer (PCa) cells to metastasize to bone, as happens in over 95% of lethal cases, cells must migrate through at least five perlecan-rich extracellular matrix (ECM) layers including the sub-epithelial BM, the endothelial BM at both origin and exit and the territorial matrices in glandular connective tissue and upon arrival in bone marrow. The over 4000 amino acid long perlecan protein core, which constitutes an innate tissue border (Farach-Carson et al., 2013), also binds growth factors (GFs) such as platelet derived GF whose release by proteolysis can occur during wound healing (Gohring et al., 1998), or sonic hedgehog whose association with perlecan core and glycosaminoglycan (GAG) chain enhances PCa growth and metastasis (Datta et al., 2006). Perlecan's interaction with growth factors and receptors is crucial in both normal development and in disease progression. Perlecan in cartilage modulates vascular endothelial growth factor receptor-2 activity to allow vascular invasion for endochondral bone formation (Ishijima et al., 2012). Meanwhile, perlecan in synovial fluid positively regulates TGF-β signaling to induce osteophyte formation in mouse osteoarthritis models (Kaneko et al., 2013). An intriguing idea is that perlecan, when intact, serves as a tissue barrier and GF reservoir that is readily available during wound responses to limit cell mixing and to mount an immediate GF-mediated tissue healing response (Farach-Carson et al., 2013). To maintain their unregulated growth, cancer cells including PCa cells can hijack this wound healing response to feed themselves constantly from the HS-bound GF reservoir bound to perlecan in the ECM, an action that involves the GF-liberating action of heparanase (Reiland et al., 2004). Additionally, as the tumor mass expands and invades the surrounding tissue in early stages of metastasis, perlecan must be cleaved and degraded in the underlying epithelial BM, in reactive stroma ECM (Warren, 2013) and in the vascular BM to allow intravasation to occur. While this perlecan turnover clearly involves the enzymatic activity of PCa proteases and GAGases such as heparanase and sulfatases (Brown et al., 2008; Lamanna et al., 2008), the proteases that cleave perlecan have not been identified in the context of PCa invasion.

Previous studies have found perlecan to be relatively resistant to proteolysis, although several extracellular proteases including matrix metalloproteinase 3 (MMP-3) (stromelysin-1), membrane type 1 (MT1)-MMP, MT2-MMP, and collagenase-1 can cleave

perlecan to varying extents (d'Ortho et al., 1997; Whitelock et al., 1996). Two proteases, cathepsin L and BMP-1, are responsible for specifically cleaving Dm V to produce endorepellin/LG3/Dm V (Iozzo et al., 2009), but do not digest perlecan completely. Not all extracellular proteases cleave perlecan, which resists cleavage by the gelatinases MMP-2 and 9 (Whitelock et al., 1996). MMP-2 and 9 are strongly associated with invasive cancer potential; so their inability to cleave perlecan suggests another protease is primarily responsible for cleaving perlecan during cancer progression. An important extracellular protease in PCa invasion is matrilysin or MMP-7, although its ability to cleave perlecan has not been examined. Expression of MMP-7 mRNA was found to be upregulated in primary and invasive PCa (Pajouh et al., 1991). Protein expression of MMP-7 and its inhibitor, tissue inhibitor of metalloproteinase-1 (TIMP-1), reveals a higher MMP-7 to TIMP-1 ratio in more advanced PCa versus localized PCa or benign prostatic hyperplasia, indicating that the enzyme is active in invasive PCa tissue (Hashimoto et al., 1998). Interestingly, immunohistochemistry studies showed increased MMP-7 stromal deposition in high grade PCa and bone marrow metastatic lesions (Cardillo et al., 2006; Hart et al., 2002). When transfected with MMP-7, DU-145 PCa cells showed enhanced invasiveness after intraperitoneal injection into immunodeficient mice (Powell et al., 1993).

MMP-7 is a secreted MMP consisting of a catalytic and activation blocking pro domain. The specificity matrix of 180 reported substrate cleavages in MEROPS (http://merops.sanger.ac.uk) reveals that the only defining feature of MMP-7 is its general preference for a leucine in the P(1)' site (Turk et al., 2001; Welch et al., 1996), which has been shown previously using tropoelastin as substrate (Heinz et al., 2010). While the MMP-7 ECM substrate specificity has been investigated (Amalinei et al., 2007; Welch et al., 1996), it has been impossible to predict if perlecan possesses sites subject to MMP-7 cleavage. However, MMP-7 is a strong candidate for perlecan proteolysis because the protease generally cleaves cartilaginous proteoglycans (Woessner and Taplin, 1988), is activated by certain heparin moieties that may be similar in perlecan (Ra et al., 2009; Yu and Woessner, 2000), and cleaves aggrecan, a chondroitin sulfate (CS) proteoglycan (Fosang et al., 1992).

In studies described in this paper, we used biochemical and *in silico* approaches to determine if MMP-7 was a likely candidate enzyme to cleave perlecan during cancer cell tissue invasion. Susceptibility to cleavage was tested with purified perlecan, various recombinantly expressed subdomains of perlecan and with perlecan bound to other proteins in the context of the BM. The identification of discrete fragments from immunoglobulin (Ig) repeat domain IV (Dm IV), thought to be an essential component of the perlecan tissue barrier (Farach-Carson et al., 2013) was sought. Finally, we performed experiments to determine if MMP-7 cleavage of perlecan and the BM not only destroyed the barrier, but also created perlecan fragments with properties that could support PCa cell invasion.

2. Results

2.1. MMP-7 is predicted to cleave perlecan

MMP-7, an enzyme that is active in PCa progression and a candidate to cleave perlecan under physiologically relevant conditions, was subjected to *in silico* digestion using free

online Site Prediction software (Verspurten et al., 2009). Figure 1A shows the predicted cut sites in numbered rank of Average Score, a score related to the similarity of a known cut site (all predicted sites shown have >99% specificity) and the amino acid cleavage site. A majority of the predicted cut sites occur in Dm III and Dm V, with only three sites predicted to be cleaved within Dm IV. A Site Prediction MMP-7 digest including the sequence within perlecan Dm IV alone produced only 5 of the 20 predicted sites with specificity greater than 99% (not shown). Therefore, other parts of the perlecan core protein not in Dm IV are predicted to have preferable MMP-7 cleavage sites *in silico*, which, if accurate, would release Dm IV fragments.

2.2. Full length perlecan is a substrate of MMP-7

Given the many MMP-7 cleavage sites in the perlecan core protein predicted by *in silico* analysis, we investigated the enzyme's true *in vitro* ability to digest intact full length, HS-decorated perlecan. To do this, perlecan was purified from media conditioned by WiDr cells and either directly incubated with MMP-7, or pre-digested with heparitinases and chondroitinase (H/C) to remove the HS and/or CS chains and then incubated with MMP-7 for 2.5 hours. The western blot for detection of perlecan (antibody A71) shown in figure 1B demonstrates that perlecan is susceptible to MMP-7 cleavage even when fully decorated with HS/CS. A time-course digestion of perlecan, as shown in figure 1C, produced certain fragments originating in Dm IV (black arrows) detected using a Dm IV specific antibody, 3135. Because cancer cells degrade perlecan in the context of the other proteins in the BM that might protect against digestion by MMP-7, we conducted experiments to use MMP7 to degrade perlecan entrapped in whole BM preparations. We used human BM extract rather than murine sourced Matrigel® to avoid issues with the mouse A71 antibody and better correlate with the human perlecan and recombinant fragments tested in this study. Human BM extract was allowed to polymerize at RT and then incubated with MMP-7 over an 8 hr period. Figure 2 displays a silver stain (2A, left), a western blot with Dm I-specific A71 (2B, center) or Dm IV-specific 3135 antibody (2C, right) that were performed to detect perlecan after either control or MMP-7 digestion. Of note, the rat Dm IV antibody A7L6 works well with dot blot during purification, but does not work consistently with western blots. Moreover, A7L6 binds the first 7 Ig repeats of Dm IV (IV-1) (data not shown), while 3135 binds the last 7 Ig repeats of Dm IV (Dm IV-3). The silver stain demonstrates that many proteins are present in the BM extract and that various bands are created/destroyed over time (for example those in white boxes) by MMP-7 digestion, indicating that MMP-7 can cleave BM proteins even when they are in association with one another. Especially noted is the removal of a smeary high MW protein(s) (black arrowhead), which migrates in the same region as fully HS/CS-decorated perlecan in this system. The western blot of the same samples shown in 2A indicated new bands of perlecan (black arrows) were produced during the time course of MMP-7 digestion, possibly derived from the ~190 kDa band (white arrow). The smeary protein above the 200 kDa marker also disappeared with increasing MMP-7 incubation time (black arrowhead). Various fragments are detected when blotting for Dm IV as shown in figure 2C. It is of interest that the Dm IV antibody better detects the large diffuse band that was lost during incubation with MMP7 than the A71 antibody, which poorly detects glycosylated forms of perlecan. Similar sized fragments were detected during digestion of BM as was found in full length perlecan digestion (black arrows). Taken

together, these experiments showed that *in vitro*, full length perlecan is a ready substrate for MMP-7 both in its purified state and in a BM matrix in the context of its BM binding partners.

2.3. MMP-7 digests every subdomain of perlecan Dm IV

Dm IV of perlecan consists of 21 Ig repeats that are non-uniform and represent distinct Ig module subtypes (Farach-Carson et al., 2013). The *in silico* digest prediction suggested that Dm IV of perlecan is largely devoid of consensus MMP-7 proteolytic sites, yet this domain encompasses nearly half of the molecule's length. To determine the susceptibility of Dm IV to MMP-7 digestion, human perlecan Dm IV was cloned, expressed as individual recombinant proteins, and purified as three separate modules each consisting of 7 Ig repeats (Dm IV-1, 2, 3) and as a sub-part of IV-3, Dm IV-3a that we previously showed to contain an adhesion promoting motif (Farach-Carson et al., 2008).The schematic of the subdomains we created is outlined in figure 3A. Each recombinant protein was incubated individually with MMP-7. Figure 3B displays a silver stained gel of each subdomain alone or after incubation with MMP-7. Every subdomain of perlecan Dm IV was found to be susceptible to MMP-7 cleavage, producing a downshift and several new bands not present in the control digest. Dm IV-3a was purified as a smaller part of Dm IV-3, and even this produced a single downshifted band near the 38 kDa marker. This band mirrors the same fragment found in digested intact perlecan and in the BM when blotted for perlecan Dm IV with 3135. This antibody binds in the same region for Dm IV-3 or IV-3a. Interestingly, expressed Dm IV-3 and IV-3a have additional glycosylation, producing a smeary purification product. Digestion with an endoglycosidase, PNGase F, caused a slight downshift, but the smeary band remained (data not shown), indicating other forms of glycosylation or post-translational modifications exist. MMP-7 produces similar size fragments. These experiments provide further evidence that MMP-7 is remarkable in its ability to digest perlecan and that it can specifically produce Dm IV peptides whose size is consistent with those from either full length perlecan or perlecan-rich BM digestion.

2.4. PSA, hepsin, FAP have limited specificity for perlecan

Other proteolytic enzymes related to PCa also were tested for their ability to cleave intact perlecan or perlecan domains. Prostate specific antigen (PSA), hepsin and fibroblast activation protein (FAP) were tested on different portions of perlecan core protein and the results are shown in figure S1. The enzymes tested failed to cleave full length perlecan or Dm IV-1, 2, or 3 when perlecan and protease were incubated alone (not shown). However in the findings shown in figure S1A, the His Tag antibody western blot of Dm IV-3a alone, after incubation with MMP-7, hepsin, or PSA showed that MMP-7 completely digested IV-3a, but PSA and hepsin each created slightly downshifted bands. This indicates that MMP-7 cleaves at the C-terminus (removing the polyhistidiine tag) and PSA and hepsin digest IV-3a at the N-terminus, conserving the polyhistidine tag. While FAP alone displayed no ability to cleave perlecan Dm IV-3 (figure S1B, lane 4), FAP digestion combined with MMP-7 produced new bands (boxed portion in lane 5) not observed with MMP-7 alone (lane 3). The experiment was repeated to verify the two additional boxed faint bands. Also note that FAP migrates near the same molecular weight as Dm IV-3 in these gels, and is not due to presence of undigested Dm IV-3 or improper loading. Therefore, other PCa proteases

may be able to further cleave perlecan once it has been fragmented by more robust proteases, such as MMP-7, to unveil cryptic proteolytic sites.

2.5. Identification and characterization of perlecan Dm IV-3 sites of cleavage by MMP-7

To determine the representative MMP-7 site specificity for perlecan, a mixture of MMP-7 digested perlecan Dm IV-3 was analyzed by N-terminal sequencing, Matrix-assisted laser desorption/ionization mass spectrometry (MALDI MS), and liquid chromatography MS (LC-MS). Figure 4 presents a summary of the identified limit fragments produced by MMP-7 digestion of intact perlecan. In figure 4A, perlecan Dm IV-3 was digested with MMP-7 and the resultant polyvinylidine fluoride (PVDF) membrane was stained with Coomassie to reveal five major bands that were subjected to N-terminal sequencing. This fragmentation banding pattern was the most common seen in multiple experiments, hence was used in analysis. We observed that the patterns seen were altered by differences in digestion time, enzyme to substrate ratios, and method of detection, as expected for an enzyme digestion. These variations account for the slight variances in patterns seen between figure 3 and supplemental figure S1. A schematic in figure 4B shows the cleavage products that were created for each band by taking into account the approximate MALDI MS discriminated mass and smaller peptides found through LC-MS. MALDI generated peaks are in supplemental data figure S2, and confirmed LC-MS peptides are mapped out in supplemental figure S3 and supplemental table S1. Note that APLD (written in italics) is the beginning of the recombinant protein as a part of the BM-40 signal sequence; the actual perlecan Dm IV-3 sequence begins at PSEG which was sequenced in bands 4 and 5. Additionally, full length Dm IV-3 only has a predicted MW of 75.46 kDa, yet the MALDI data indicates an intact MW of approximately 79.2 kDa. Therefore, matching predicted MW and protein fragment was not exact because the post translational modification makes sizes vague by approximately 4 kDa. However, the fragments laid out in figure 4B likely represent the largest fragments generated by MMP-7. Fragments range from approximately 17 kDa to 53 kDa, and several of the bands represent Dm IV-3 internal cleavage sites, meaning both the C and N-termini can be deciphered reasonably. Data from the LC-MS peptides and the N-terminal sequencing indicate MMP-7 has a strong preference for aliphatic amino acids at the P1 site, generating mostly leucine (25 sites), valine (6 sites), isoleucine (5 sites), or alanine (3 sites) at the N-terminal sites in Dm IV-3. The C-termini do not seem to require the presence of any particular amino acid, but the most common amino acid at the P1 site is glutamine. Additionally, PHYRE modeling suggests that cut sites (shown as red in figure 4B) appear in the unstructured transitions between Ig modules (Ig20 and 22) and between connections to the interfacing beta sheets (Ig17). Further validating the N-terminal sequencing data, the heptapeptide LEQRTYG (highlighted as red in the Ig17 model in figure 4b) appeared in LC-MS data, which would be generated when MMP-7 cleaved perlecan at those N-terminal sequence identified regions. Performing a Site Prediction analysis on the sequence of recombinant Dm IV-3 produces 20 predicted sites, albeit with much lower Specificity percentage than full length perlecan (not shown). Interestingly, only six of the predicted sites match the peptide cleavage sites found through MS and N-terminus sequencing data. Band 3 is a common fragment produced by MMP-7 regardless of how perlecan is presented. In supplemental figure S4, BM extract, purified perlecan, Dm IV-3, and WiDr concentrated conditioned media (the source of full length

perlecan in this study) were digested with MMP-7 overnight. Each produced a similar fragment below 41 kDa and is detected by antibody 3135. Also note that bands 4 and 5 from figure 4A are not detected with antibody 3135 (lane 6), which coincides with the epitope range of 3135. Taken together, the combined data clearly shows that MMP-7 cleaves Dm IV of perlecan with non-predicted site specificity, and by doing so creates multiple small peptides and larger internally cleaved fragments some of which are post-translationally modified.

2.6. MMP-7 effects PCa cell invasion through BM matrix

To test the potential pro-metastasis effects of MMP-7, a Transwell® invasion assay through perlecan-rich human BM was utilized. BM extract was incubated in serum free media with MMP-7 to ensure that similar results were matched to the time course digestion shown in figure 2C, which included cell culture incompatible Triton X-100. Figure 5A demonstrates that even in cell culture media without any detergents, perlecan was cleaved efficiently and similarly to previous experimental conditions. Additionally, the same sized perlecan Dm IV fragments were generated in cell culture conditions. Figure 5B–D show representative images from an 80 hr C4-2 cell invasion assay through a BM extract coated 8 μm pore polycarbonate membrane. Panel B shows cells that migrated through membrane that contained BM extract only (condition 1), panel C is BM predigested with MMP-7 and coated (condition 2 in figure), and panel D is coated BM subsequently digested with MMP-7 (condition 3). As quantified in panel E, invasiveness through BM is enhanced if perlecan-rich BM is digested with MMP-7. In this experiment, invasion through the polycarbonate membrane was increased regardless of whether the coated BM extract was predigested with MMP-7 or was digested after the BM was coated onto the membrane, but was greatest when BM was digested after assembly. Overall, this experiment demonstrates that MMP-7 activity creates holes in the BM that allow C4-2 cells to break through the barrier normally associated with the perlecan-rich BM border.

2.7. MMP-7 affects the ability of perlecan Dm IV-3 to cluster PCa cells

Dm IV-3 represents at least one of the modules of perlecan that creates discrete large fragments after MMP-7 digestion. We investigated the effects of Dm IV-3 on the behavior of two invasive PCa cell lines, PC-3 and C4-2. While coating dishes with other recombinant generated subdomains IV-1 and IV-2 did not produce marked effects on cells (not shown), coating with Dm IV-3 produced a striking clustering effect as seen in figure 6A using C4-2 cells. A similar effect was seen with the PC-3 cells in the presence of Dm IV-3 (figure 6C), but to a somewhat lesser extent than seen with C4-2 cells. However, clustering was cell-type specific. For example, HS5 bone marrow stromal cells did not cluster at all on Dm IV-3 (data not shown). We controlled for general non-adherence by coating bovine serum albumin (BSA) at the same concentration as Dm IV-3. However, BSA at this low concentration did not induce clustering of any type. Plates coated with high concentrations of BSA resulted ultimately in dead floating single cells (data not shown). For both cell lines, predigestion of Dm IV-3 with MMP-7 abrogated the clustering effect, favoring cell dispersion and spreading as seen with either BSA controls or other perlecan fragments. Quantification of the cell dispersion/spreading versus clustering behavior shown in figures 6E and F clearly demonstrates the strong clustering effect of Dm IV-3, and further that

MMP-7 cleavage of Dm IV-3 destroys its clustering activity. To understand the context specific activities of soluble and substratum-fixed Dm IV-3, we carried out the experiments shown in figure 7. Plates pre-coated with Dm IV-3 were simultaneously seeded with C4-2 cells and a digestion mixture of either control BSA, MMP-7 and BSA, IV-3, IV-3 and MMP-7, or the Dm IV peptide used in previous studies (Farach-Carson et al., 2008). Dm IV-3 with control BSA produced clustered cells, as before. Soluble Dm IV-3 enhanced clustering, but only slightly. Soluble Dm IV-3 or BSA pre-incubated with MMP-7 strongly reversed the Dm IV-3 induced clustering in comparison to control BSA and IV-3. The PCa pro-adhesive peptide (Dm IV peptide that lies within Dm IV-3) did not counteract the effects of Dm IV-3 as a cluster inducing substrate. Together, these experiments provide evidence that Dm IV-3 induces positive clustering effects on PCa cells and that MMP-7 activity reverses this to favor cell dispersion and spreading normally associated with cancer.

3. DISCUSSION

The overall goals of this study were to identify proteolytic enzymes present in the tumor microenvironment that could be responsible for cleavage of perlecan in matrices, and to determine what, if any, cellular behaviors are influenced by perlecan processing. A likely candidate proteolytic enzyme able to cleave perlecan was MMP-7 or matrilysin. MMP-7 expression and activity have been well linked to cancer and PCa, specifically (Cardillo et al., 2006; Hart et al., 2002; Hashimoto et al., 1998; Lynch et al., 2005; Powell et al., 1993). MMP-7 has many demonstrated ECM substrates including collagen I, III, IV, V, fibronectin (Woessner and Taplin, 1988), vitronectin (Imai et al., 1995), and aggrecan (Fosang et al., 1992). MMP-7 may dissolve the BM well *in vivo*, but its ability to digest perlecan, a critical BM component, to this point had been unexplored. MMP-7 earlier has been reported to digest unspecified cartilage derived “proteoglycans” (Woessner and Taplin, 1988), and we hypothesized that this might include perlecan. The *in silico* prediction’s top 18 sites ranked above 99% in Specificity, indicating perlecan was likely to be a strong substrate. The top ranked MMP-7 *in silico* digest of full length perlecan predicted cleavage to favor production of large Dm IV fragments, which was subsequently verified using either BM or intact perlecan as substrates for digestions.

Current *in vitro* experiments verified the substrate recognition of full length perlecan by MMP-7. Unlike other MMPs such as MMP-3/stromelysin (Whitelock et al., 1996), MMP-7 can extensively cleave perlecan even with the HS/CS chains intact. The lack of GAG chain inhibition also was observed with aggrecan, which is cleaved by MMP-7 in the keratan sulfate rich interglobular domain (Fosang et al., 1992). The ability to digest perlecan with intact GAG chains might have been predicted because MMP-7 binds to and is activated by highly sulfated heparin-like regions potentially found on perlecan (Ra et al., 2009; Yu and Woessner, 2000). Therefore, perlecan GAG chains potentially could serve as an available docking site for efficient proteolysis during cancer invasion, releasing cryptic fragments and GFs associated with perlecan’s protein core and HS/CS chains. In the context of the BM, our new data suggests perlecan is cleaved from the C-terminus inward given the continued recognition by the domain I antibody, which was not observed when perlecan was incubated alone with MMP-7. Earlier reports that the C-terminus of perlecan is exposed more in the BM lattice at the stromal interface add credence to the results (Heremans et al., 1989).

Additionally, MMP-7 releases Dm IV positive fragments either when incubated with intact perlecan or perlecan in the BM complex. Interestingly, the fragments are nearly identical in apparent molecular weight despite the different presentation. Supplemental figure S4 suggests that the most commonly shared fragment from each digestion type (BM, full length perlecan, Dm IV-3, and conditioned media) is below 41 kD, and that it correlates strongly to band 3 from figure 4. While placental BM extract has detectable Dm I and Dm IV positive smeary bands that disappear upon MMP-7 incubation, the primary tight band is slightly below 200 kDa. Unknown is whether this perlecan band represents a pre-digested product or a potentially novel variant perlecan form specific to placental tissue. Regardless, the experiment demonstrates that perlecan fragments are generated by MMP-7 activity even when perlecan is bound into a complex BM network. Invasive cancers, including PCa, degrade ECM proteins in the BM and in tissues and in the process may release perlecan fragments. Especially interesting will be determining if perlecan fragments increase in patients with early metastatic bone lesions, given the considerable presence of perlecan in bone marrow (Klein et al., 1995). Such studies are ongoing.

The proteolytic release of perlecan derived fragments also is significant to several biological processes beyond cancer cell invasion through perlecan-rich matrices (Iozzo et al., 2009). As a proteomic screen for premature rupture of amniotic membranes, a 19 kDa fragment of perlecan was found only in the amniotic fluid but not the maternal blood of pregnant females (Vuadens et al., 2003). Additionally, a C-terminal fragment of perlecan was found in the follicular fluid, but not serum, of women undergoing successful *in vitro* fertilization (Jarkovska et al., 2010). A 25 kDa C-terminal fragment of perlecan also was found in urine of hemodialysis patients with end stage renal failure (Oda et al., 1996). Even a 90 kDa fragment derived from perlecan Dm IV is high in the vitreous humour and serum of a chick embryo, but rapidly disappears upon hatching (Balasubramani et al., 2004). By far the most studied bioactive perlecan fragment is Dm V/LG3/endorepellin (Mongiat et al., 2003) that is released by the proteases BMP-1 and cathepsin L (Cailhier et al., 2008; Gonzalez et al., 2005). The bioactive fragment affects angiogenesis by modifying the behavior of endothelial cells and vascular smooth muscle cells (Bix et al., 2004). Also, following ischemic stroke in a rodent brain model, perlecan Dm V is proteolytically released to mediate angiogenesis ultimately being neuroprotective (Lee et al., 2011). These studies demonstrate perlecan as an intact molecule can induce distinctly different behaviors than do its protease produced fragments, consistent with the findings of the current study with MMP-7. Perlecan degradation and fragment release may be common to basic development and pathologies involved with ECM turnover and it will be interesting to explore further the contribution of Dm IV fragments.

Every subdomain of Dm IV was found to be susceptible to MMP-7 digestion despite the lack of predicted high confidence cleavage sites. This finding re-emphasizes that MMP-7 has promiscuous substrate specificity, potentially more dependent upon interaction with the 3D protein structure than the specific primary substrate sequences. Other extracellular proteolytic enzymes were incubated with perlecan, but MMP-7 was the only enzyme with high proteolysis ability directed toward perlecan. In fact, none of the other enzymes tested (PSA, hepsin, and FAP) cleaved intact perlecan with or without its HS chains. FAP is a

protease upregulated in reactive stroma surrounding prostatic intraepithelial neoplasias and PCa tumors (Tuxhorn et al., 2002), but only a short list of physiological substrates exists (Kelly et al., 2012). FAP only was able to produce fragments on a specific domain of perlecan in combination with MMP-7. Similarly, FAP only is able to produce collagen I and III degradation peptides after pre-digestion with MMP-1 (Christiansen et al., 2007). PSA degrades some ECM components including laminin and fibronectin (Webber et al., 1995), but this is the first report of perlecan as a weak substrate. However, the recognition is only of a small portion of perlecan, indicating that prior digestion by another proteolytic enzyme is likely to be necessary. The same may be true of hepsin, which downshifted Dm IV-3a migration only very slightly. Hepsin has a confirmed ECM molecular cleavage site within laminin-322's β-3 chain (Tripathi et al., 2008). The resulting hepsin-generated laminin fragment induced migration in LNCaP cells (Tripathi et al., 2008). In this regard, it may be possible for hepsin to release cryptic fragments of perlecan if the right substrate is presented. Overall, this demonstrates that MMP-7 can efficiently cleave perlecan, and its action may generate new substrate peptides for other extracellular proteases to digest. Based on this evidence, we propose that MMP-7 remains the strongest candidate responsible for the *in vivo* perlecan BM and stromal matrix destabilization necessary for cancer invasion and migration to occur during metastasis.

The site specificity of MMP-7 for perlecan falls in line with the established specificity matrix found in the MEROPS database (http://merops.sanger.ac.uk/cgi-bin/pepsum?id=M10.008). Notably, MMP-7 has the same preference for leucine in the P1 site, and a slight preference for glutamine at the P1 site and for proline at the P2 site in perlecan as reported in MEROPS. Multiple bands with the same N-terminus as in bands 1, 2 and 3 suggest perlecan is sequentially degraded by MMP-7, perhaps preferentially cutting at the N-terminus sequenced site and degrading from the C-terminus inward to create sub fragments. In the process, multiple peptides in the 5–20 amino acid range are released. Testing the biological effects (e.g. adhesion, motility, and chemotaxis) of these specific peptides and protein limit fragments on cells related to PCa, including the LNCaP derived cell line, bone stromal cells, and immune surveillance cells will be done in follow up studies to this work. PHYRE modeling reveals that MMP-7 initially may cleave at transition areas (between Ig repeats and between beta sheets) to reveal additional sites for cleavage. This type of preference suggests that perlecan Dm IV is tightly structured and needs to be loosened before additional cleavage can occur, which coincides with mouse Dm IV structure observed through rotary force shadowing (Hopf et al., 1999). Additionally, we found discrepancies between the expected and observed MW of Dm IV-3 by approximately 4–5 kDa. Likely, Dm IV-3 is O- or N-glycosylated but not decorated with GAG chains as was determined previously in mouse derived Dm IV (Hopf et al., 1999).

The ability of MMP-7 to destabilize the BM and increase the invasive/migratory capacity of C4-2 cells must involve perlecan degradation. Perlecan acts as an organizer of the BM matrix, linking together collagen, laminin, and nidogen into a network (Behrens et al., 2012; Farach-Carson et al., 2013). With perlecan degraded by MMP-7, the matrix is expected to be compromised, providing an escape route for invasive cancer cells. Besides a mechanical border, perlecan degradation creates cryptic bioactive fragments. It is likely that MMP-7

acts upon perlecan in a fashion similar to that by which MMP-2/gelatinase acts upon laminin-5. MMP-2, which does not effectively cleave perlecan, cleaves laminin-5 exposing a pro-migratory cryptic site that induces breast cancer cells (MCF-7) to become motile (Giannelli et al., 1997). MMP-7 processes other ECM proteins to generate bioactive protein fragments, such as neostatin-7 derived from collagen XVIII (Chang et al., 2005). The same phenomenon is likely to occur during MMP-7 perlecan fragmentation.

We found that Dm IV-3 of perlecan induced a strong clustering effect when presented as a fixed substratum. The effects were observed with two PCa cell lines. The poorly adherent C4-2 clusters are highly reminiscent of C4-2B cell morphology that was observed previously in 3D hyaluronic acid based hydrogels (Gurski et al., 2009). The effect is unlikely to be entirely from non-adherence, given that BSA, a non-adherent protein, adsorbed to plates did not induce this clustering when present at the same concentration. Moreover, other subdomains, IV-1 and IV-2, did not produce this strong clustering effect. Our findings that MMP-7 digestion reverses the clustering effect of Dm IV-3 hints that a receptor/Dm IV-3 complex that induces the clustering may exist. We are currently investigating the functions of the various fragments and peptides produced by Dm IV-3 degradation by MMP-7. Previously, an 18 amino acid peptide from Dm IV was found to have pro-adhesive and FAK activating properties on certain cell types (Farach-Carson et al., 2008). Dm IV-3 contains this peptide, specifically after the N-terminal sequenced amino acid cleavage site 3481 in figure S3. Adding this peptide in solution when seeding cells, however, did not overcome the pro cell-cell contact induction by intact Dm IV-3. This suggests that there is a strong pro-clustering peptide sequence or tertiary structure that is destroyed by MMP-7 proteolysis. This is further supported by the observation that addition of soluble MMP-7 (either pre-incubated with BSA or IV-3) prevented the clustering of adsorbed Dm IV-3 on the plate. It is interesting to speculate that the switch between cell-cell clustering and cell dispersion induced by MMP-7 digestion of perlecan-rich BM may be mimicking an epithelial to mesenchymal transition occurring in these cells as they acquire invasive potential.

The degree to which MMP-7 and perlecan interact in PCa progression and metastasis remains unknown, however, in other cancers an association has been demonstrated. While oral carcinoma *in situ* has an epithelial MMP-7 expression, squamous cell carcinoma has a more stromal appearance, matching perlecan stromal expression (Tilakaratne et al., 2009). MMP-7 also shows enhanced stromal expression in higher grade PCa cancer (Cardillo et al., 2006). In chicken cornea, active wound healing stromal sites, which are analogous to reactive stroma in cancer, upregulate perlecan expression as determined by staining with a Dm IV antibody (Ritchey et al., 2011). Therefore, perlecan deposition in reactive stroma may be a widespread phenomenon. If perlecan and MMP-7 co-localize at reactive stromal sites, MMP-7 is likely to be active. PCa and reactive stromal compartments, in particular, have a high oxidative character (Josson et al., 2010; Platz and De Marzo, 2004). Oxidative species *in vitro* activate MMP-7 by removing the pro-domain inhibiting cysteine from the active site (Fu et al., 2001). Additionally, oxidative species themselves can destabilize the BM and reactive stromal proteins, including perlecan, making them more susceptible to proteases (Kennett et al., 2011). Therefore, we have initiated studies with a large number of

clinical specimens to determine if perlecan and MMP-7 co-localize in PCa tissue and expect to report on that soon.

4. Experimental procedures

4.1. Materials

The rabbit anti-human perlecan genomic antibody 3135 was generated using a proprietary technology developed at Strategic Diagnostics, Inc (Newark, DE). Antibody 3135 binds to Dm IV-3 between amino acids 3295 and 3394. Mouse anti-perlecan domain I antibody A71 was purchased from Pierce (Rockford, IL) and rat anti-Dm IV antibody A7L6 was purchased from Life Technologies (Grand Island, NY). Heparitinase I, II, III, chondroitinase ABC, and MMP-7 (cat no. M4565) were purchased from Sigma-Aldrich (St. Louis, MO). FAP was purchased from R&D Systems (Minneapolis, MN), and PSA was purchased from EMD Millipore (Darmstadt, Germany). Cultrex® placental human BM extract (cat no. 3415-001-02) was purchased from Trevigen (Gaithersburg, MD). For mass spectrometry (MS) analysis sinnapic acid matrix and trifluoroacetic acid were purchased from Sigma-Aldrich, water and acetonitrile were from J.T. Baker of Avantor (Center Valley, PA), formic acid was from Thermo-Fisher Scientific, and the Ascentis Express C-18 peptide ES column was purchased from Supelco (Bellefonte, PA). All other materials used were reagent grade or better.

4.2. Site prediction digestion of perlecan in silico

Using the free Site Prediction website (http://www.dmbr.ugent.be/prx/bioit2-public/SitePrediction/index.php) (Verspurten et al., 2009) the amino acid sequence of perlecan (uniprot ID: P98160) was subjected to *in silico* digestion by MMP-7 under default settings. Sequence cleavage specificity was extracted from the MEROPS database for MMP-7 from all organism sequences available (*Bos taurus*, 3; *Homo sapiens*, 137; *Mus musculus*, 22; *Rattus norvegicus*, 7). All sequence specificities reported are greater than 99 percent. The specificity percent as described by Site Prediction is the chance that a proteolytic site above a given threshold will actually be cleaved. Site Prediction also was performed on Dm IV of perlecan, amino acids 1677–3662 [accession no. NM_005529.5], and Dm IV-3 recombinant protein sequence (supplemental figure S3).

4.3. Perlecan purification from WiDr conditioned media

WiDr cells purchased from ATCC (cat no. CCL-218) were cultured in Eagles minimal essential media (EMEM) (ATCC) with 10% (v/v) heat inactivated fetal bovine serum (FBS) (Atlanta Biologicals, Lawrenceville, GA), 1× penicillin/streptomycin (Life Technologies) and 1× L-glutamine (Life Technologies). Cells were incubated at 37°C in a 5% (v/v) CO_2 atmosphere and passaged at 80–90% confluency. WiDr cells were described previously to produce perlecan as their primary HSPG (Fuki et al., 2000; Iozzo, 1984), thus were used as a cell factory protein source. When cells were nearly 100% confluent in Cell Culture Vessel Hyperflasks, (Corning, Tewskbury, MA) they were switched to 2% FBS media. Recovered conditioned media was processed through a 0.45 μm Stericup filter units (Millipore, Billerica, MA). Phenylmethyl sulfonylfluouride (PMSF), benzamadine, and EDTA at 0.5 mM each and 0.02 % (w/v) sodium azide were included in the conditioned media. The

solutions were processed through a S34100 Amicon spiral wound 100 kiloDalton (kDa) molecular weight cutoff media concentrator cartridge (Millipore). The resulting high molecular weight concentrated solution was subjected to diethyl aminoethyl (DEAE) anion exchange chromatography (GE Healthcare). Equilibration buffer contained 2 M urea, 50 mM PIPES pH 7.0, 250 mM NaCl, 2.5 mM EDTA, 0.5 mM benzamadine, 0.5 mM PMSF, and 0.02% sodium azide. Elution buffer was identical to equilibration buffer except the NaCl was 750 mM. Eluted 1.5 mL fractions were collected and the absorbance read at 280 nm. Fractions were analyzed individually by dot blot immunoassay with anti-perlecan Dm IV antibody A7L6 (described below). Pooled fractions containing perlecan were dialyzed in MilliQ water and centrifuged in a speed vac until the desired concentration was obtained. The resulting perlecan enriched solution was separated by Sepharose CL-4B (Sigma) gel filtration chromatography in the presence of 0.8 M NaCl PBS buffer. A perlecan peak containing immunopositive fractions was pooled, dialyzed in MilliQ water and centrifuged in a speed vac. Perlecan-rich protein pools were subjected to gradient heparin Sepharose 6 Fast Flow (GE Healthcare) chromatography in a PBS buffer containing 0.2, 0.3, 0.5, 1.0, or 1.5 M NaCl. Perlecan, as determined by A7L6 dot blot, eluted at 0.3 M NaCl. Perlecan was concentrated in a speed vac and dialyzed into a final PBS buffered working solution. Samples were aliquotted and stored at -80°C until used. Purity was assessed by silver stain as described below.

4.4. Cloning and purification of Dm IV constructs

Dm IV of perlecan (21 Ig repeats enompassing amino acids 1677–3662 and cDNA base pairs 5029–10986 [accession no. NM_005529.5]) was recreated and expressed using recombinant technology as three separate pieces, each containing 7 Ig repeats. Linking regions between Dm IV-1, Dm IV-2, and Dm IV-3 were determined by Protein Homology/analogY Recognition Engine version 2.0 (PHYRE V2.0) (http://www.sbg.bio.ic.ac.uk/~phyre2/html/page.cgi?id=index) (Kelley and Sternberg, 2009). Dm IV was divided at these points to avoid disrupting Ig module folding. WiDr mRNA was collected with Trizol Reagent (Life Technologies) according to manufacturer's directions. Monsterscript 1st-Strand cDNA Synthesis Kit (Epicentre, Madison, WI) (Cat no. MS040910) with random nonamer primers was used to generate the cDNA. Dm IV-1 (Ig repeats 1–7, amino acids 1677–2338, base pairs 5029–7014) was cloned into a vector similar to pCEP-pu (Life Technologies) containing a CMV promoter, a BM40 signal sequence for secretion, and a C-terminal V5 tag and poly histidine tag. The vector also contains an internal ribosomal entry site for a green fluorescent protein sequence and a separate puromycin resistance for selection in mammalian cells. Dm IV-1 PCR products were amplified with flanking Nhe1 and Not1 restriction sites, separated and excised from an agarose gel, and ligated into the vector after digestion with Nhe1 and Not1 restriction enzymes (New England Biolabs, Ipswich, MA). An enterokinase cleavage site sequence was introduced through two rounds of site directed mutagenesis with a QuikChange II XL kit (Agilent Technologies, Santa Clara, CA). Dm IV-2 (Ig repeats 8–14, amino acids 2338–3010, base pairs 7012–9030) was synthesized by GENEWIZ (South Plainfield, NJ) and cloned into the same vector as Dm IV-1. Dm IV-3 (Ig repeats 15–21, amino acids 3011–3662, base pairs 9031–10986) PCR products were amplified with a forward BM40 signal sequence and a reverse primer flanked with an enterokinase site, inserted into a pENTR/D-TOPO entry vector (Life Technologies)

and transferred to a pcDNA-Dest40 mammalian expression vector (Life Technologies). Dm IV-3a, a subpart of Dm IV-3, is the peptide between amino acids 3126–3408 (base pairs 9376–10224). This was cloned similarly to Dm IV-1, except an enterokinase site was not included. Sequence verified vectors containing Dm IV were transfected into human embryonic kidney 293-Adherent (HEK293-A) cells (Life Technologies) with Lipofectamine 2000 transfection reagent (Life Technologies). After antibiotic selection (Dm IV-1, Dm IV-2, Dm IV-3a: 400 ng/mL puromycin; Dm IV-3: 1mg/mL Geneticin, Life Technologies) in DMEM, 10% FBS, 1× penicillin/streptomycin (Life Technologies), 1× L-glutamine (Life Technologies), serum free conditioned media was collected. Conditioned media was processed through a Stirred Cell Millipore media concentrator with a 10,000 Dalton cutoff concentrator filter. Nickel chromatography with Ni-NTA agarose resin (Qiagen, Valencia, CA) was performed on the concentrated conditioned media and eluted with 300 mM imidazole 50 mM sodium dihydrogen phosphate, 300 mM sodium chloride, and 0.05% (v/v) Tween-20, pH 8.0. Equilibration and wash buffers were identical, but instead contained 10 mM and 20 mM imidazole, respectively. Appropriate fractions were concentrated and buffer exchanged to remove imidazole using Millipore Amicon Ultra Centrifugal Filters (Ultra Cel-50 kDa MWCO membrane, cat no. UFC505024).

4.5. Enzyme digestion of perlecan, perlecan Dm IV, and placental BM extract

Perlecan and perlecan Dm-IV were subjected to enzymatic digestion by MMP-7, as well as PSA, FAP and hepsin, three other proteases common to the prostate (Kelly et al., 2012; Tripathi et al., 2008; Webber et al., 1995). Perlecan was incubated at varying enzyme to substrate ratios as noted in the results for individual experiments. For basic MMP-7 digestions, the buffer contained 10 mM HEPES buffer pH 7.0, 3 mM calcium acetate, and 1 mM EDTA. For placental BM extract proteolysis (6 μg per 0.2 μg MMP-7 in 40 μl total), the MMP-7 digestion buffer was identical, but lacked Triton X-100. Additionally, time points for BM extract digestion were stopped with 2.5 mM final EDTA and allowed to depolymerize at 4°C before subsequent processing. During MMP-7 co-incubation with FAP, all buffers were identical and contained 50 mM Tris-HCl pH 7.5, 150 mM NaCl, 3 mM calcium chloride, and 0.1% (v/v) Triton X-100. For a FAP positive control, 10 mg of rat tail collagen type 1 (Sigma, cat no. C7761) was dissolved in 10 mL 0.1 M acetic acid for 1 hr at room temperature (RT) and heat denatured at 68°C for 24 hrs before digestion with MMP-7 and FAP. Hepsin digestion (0.5 μg per 6 μg perlecan construct in a 30 ul reaction volume) was attempted using two conditions; 30 mM Tris HCl, pH 8.4, 200 mM NaCl, 0.1% (v/v) DMSO and alternately 50 mM Tris HCl, pH 7.5, 250 mM NaCl. PSA (2 μg per 6 μg perlecan peptide in a 30 ul reaction volume) digestion buffer contained 50 mM Tris-HCl, pH 7.9, 10 mM NaCl, 0.01% Tween 20. All were incubated at 37°C for varying times noted in results. Heparitinase I, II, III and chondroitinase ABC digestions of full length perlecan were performed in PBS, pH 7.4 with 2 mM calcium chloride at 0.1 units (as defined by Sigma) per enzyme and 20 μg of perlecan in a reaction volume of 40 μL at 37°C for at least 6 hrs.

4.6. Western blot, dot blot, and silver stain

For purified perlecan, digestion reactions and controls were denatured at 99°C with reducing sample buffer (final 60 mM Tris-HCl, 1% (w/v) sodium dodecyl sulfate (SDS), 10% (v/v) glycerol, 2% (v/v) 2-mercaptoethanol, pH 6.8 with tracking dye) for 5–10 min. Samples

were separated with SDS-polyacrylamide gel electrophoresis (PAGE) in 1 mm Novex NuPAGE 4–12% polyacrylamide gradient bis-tris buffered gels (Life Technologies) in a Novex NuPAGE system (Life Technologies) with 1× MOPS SDS buffer (Life Technologies) at 150 constant volts for approximately 80 min. See Blue +2 molecular weight marker (Life Technologies) and Broad Range Marker (BioRad) were used to determine apparent molecular weights. Silver staining was performed with the Silverquest Silver Stain kit (Life Technologies) according to manufacturer's directions. For western blots, separated protein was transferred to 0.45 μm pore nitrocellulose (Bio-Rad, Hercules, CA) in a tris-glycine buffer at 40 volts for 5 hr. Membranes were blocked in 3% (w/v) BSA tris buffered saline with 0.05% Tween-20 (TBST) for 2 hrs at RT. A71 antibody (200 ng/ml, 1:1000) or antibody 3135 (1:10,000) was added to the block solution overnight on a 4°C shaker. Following three by 5 min TBST washes, the membranes were incubated with 1:200,000 sheep anti-mouse HRP conjugated antibody (Jackson) in 3% BSA TBST for 2 hr at RT. Blots were washed again and incubated with chemiluminescence substrate (West Dura extended substrate, Pierce) for 5 min and exposed to film. For perlecan dot blots, 20 ul of sample was added to a BioRad slot blot apparatus and allowed to bind a pre-PBS rinsed 0.45 μm nitrocellulose membrane for 2 hr at RT. After vacuum suction, the dot blot was placed into BSA blocking solution and processed identically as the A71 western blot, except a 1:5,000 A7L6 antibody was used.

4.7. N-termini protein sequencing of perlecan cleavage sites by MMP-7

Dm IV-3 recombinant protein was incubated with MMP-7 overnight as described above and the digestion products separated by SDS-PAGE as described above. The protein was transferred to a methanol pre-soaked 0.22 μm pore PVDF membrane in 25 mM Tris, 192 mM glycine buffer with 20% (v/v) methanol at 50 V for 5 hrs at 4°C. The PVDF membrane was washed with distilled water several times to remove glycine background, and dipped in methanol again. The membrane was stained with 0.1% (w/v) Coomassie Blue R-250 in 40% methanol, 1% (v/v) acetic acid for 1 min, and destained with 50% methanol in water solution. After extensive MilliQ water washes, the membrane was left to air dry. The membrane was sent to Midwest Analytical Inc. Protein Sequencing (St. Louis, MO) for N-terminal Edman degradation protein sequencing.

4.8. MALDI MS Analysis

MALDI MS analysis was carried out using a Bruker Autoflex II Time of Flight (ToF)-ToF (Fremont, CA) instrument. Perlecan Dm IV-3 MMP-7 digests performed without Triton X-100 were analyzed using a saturated sinnapic acid matrix that was prepared in a solvent system of 60/40 acetonitrile/water containing 0.25% (v/v) TFA. 10 μL of perlecan Dm IV-3 digest (10 ug of perlecan Dm IV) were combined with 10 μL of matrix solution, mixed and then spotted for analysis. Positive ion MALDI analysis was carried out in both the linear and reflectron modes.

4.9. LC-MS analysis

LC-MS analysis of perlecan Dm IV-3 MMP-7 digests were carried out using a Thermo-Fisher LTQ-Orbitrap Mass Spectrometer interfaced with a Shimadzu Prominence ADXR UPLC system (Columbia, MD) through an Ion Max Electrospray Ionization (ESI) source.

The LTQ-Orbitrap was operated in positive ESI mode. MS spectra were acquired at a mass resolving power (m/Δm) of 30,000. MS/MS spectra were acquired using data dependent scanning. LC separations were accomplished using a 150 mm × 1.0 mm ID, 2.7 micron Ascentis express C-18 peptide-ES column operated at a flow rate of 0.15 mL/min. Mobile phase A was 0.1% (v/v) formic acid in water and mobile phase B was 0.1% formic acid in acetonitrile. The LC gradient for the analytical separation was as follows: initial conditions 5% (v/v) B to 35% B at 32 minutes, to 65% B at 40 minutes, and to 90% B at 42 minutes. For small peptides ($m/z \leq 2500$, $z \leq 5$) data analysis was carried out using Matrix Science Mascot (Perkins et al., 1999) and mMass (Strohalm et al., 2008; Strohalm et al., 2010). For larger peptides ($m/z > 2500$, $z > 5$), molecular weights were computed using MagTran deconvolution software (Zhang and Marshall, 1998).

4.10. C4-2 and PC-3 plating experiments on perlecan Dm IV-3

C4-2 bone metastatic PCa cells were cultured as described previously (Thalmann et al., 2000; Wu et al., 1994) and cultured in T-media (Gibco) with 5% heat inactivated FBS (Atlanta Biologicals) and 1× penicillin/streptomycin (Gibco). PC-3 cells were cultured in F-12K media (ATCC) with 10% FBS, 1× penicillin/streptomycin and 1× L-glutamine (Gibco). Cells were passaged at 90% confluence and incubated at 37°C in 5% CO_2 atmosphere. In triplicate, Dm IV-3 (12.5 μg per well), MMP-7 pre-digested Dm IV-3, BSA (12.5 μg per well), or BSA incubated with MMP-7 were adsorbed to a flat bottom 12-well plate (Corning) in PBS, pH 7.4 (Life Technologies). Samples were allowed to adsorb overnight at 37° C. The remaining solution was removed, washed with PBS and replaced with full culture media. C4-2 cells were passaged with 0.25% (w/v) trypsin-0.38% (w/v) EDTA (Life Technologies) and each well seeded with 100,000 cells. Cells were placed in the incubator and viewed and imaged by phase bright field microscopy at certain time points. Three 4× objective images were taken per well providing nine different images of each substrate type. Addition of soluble digest fragments and peptide to a Dm IV-3 coated wells was performed in 96-well plates. Plates were coated as before, but with less protein (1.75 μg Dm IV-3 per well). Digests were performed overnight as described before to a final concentration of 0.5 μg/mL of substrate. C4-2 cells (7,500 per well) were seeded into the wells along with digestion mixtures or peptides to a final volume of 100 μL. Each well received 2.75 μg in 100 μL media of either BSA, BSA and MMP-7, IV-3, or IV-3 and MMP-7. The domain IV peptide (TWSKVGGHLRPGIVQSG) used in previous studies was added at 20 μg/mL (Farach-Carson et al., 2008). After 48 hrs the wells were imaged at 4× objective. Using ImageJ software, batch images were quantified for particle count, particle size, and area fraction. Cell dispersion values are equal to (particle count)/(particle size)*(area fraction). A higher value is more dispersed and a lower value is more clustered. To compare dispersion values, the cells have to be of the same type, seeded at the same density, and subconfluent when imaged. An unpaired student's T-test was utilized to determine statistical significance.

4.11. C4-2 Transwell® invasion assay

Corning Transwell® inserts (8 μm pore size, polycarbonate membrane) were coated in triplicate with 6 μg BM extract (Cultrex®) in the presence of serum free T-media in three experimental conditions. The BM extract was either coated and left undigested, pre-digested

with 0.2 μg MMP-7 for 8 hours and coated, or coated and subsequently incubated with 0.2 μg MMP-7 for 8 hrs. After a brief media wash, 30,000 cells were seeded into each Transwell® in serum free T-media in the upper chamber. In the lower chamber, 10% FBS acted as the chemoattractant. After 80 hours, the cells were fixed in cold methanol and stained with 0.1 mg/mL crystal violet in 10% (v/v) ethanol and 1% (v/v) methanol and water for several minutes. The non-invaded top cells were removed with a cotton swab. With a dissecting microscope, a 2× objective image of migrating cells was taken and quantified by Image-J. An unpaired student's T-test was used to determine statistical significance.

Conclusions

In conclusion, MMP-7 digests perlecan even with the usually inhibitory HS/CS chains intact and in the presence of other BM components, and is a prime candidate to destabilize the BM during acquisition of cancer cell invasiveness and during various stages of metastasis. Additionally, every subdomain of Dm IV, which had few predicted high specificity proteolytic sites, was extensively digested by MMP-7. Other PCa-associated proteases, hepsin, PSA, and FAP, have limited ability to digest perlecan, either requiring subdomain presentation and/or pre-digestion by MMP-7. In a cell biological context, exogenous MMP-7 degraded perlecan in BM allowing greater motility and invasion of PCa cells. Also, MMP-7 activity reversed the potent cell clustering effect by perlecan Dm IV-3, favoring cell dispersion. Taken together, these studies suggest that MMP-7 in the tumor microenvironment, perhaps acting in concert with other enzymes, can degrade perlecan in the local ECM to support disease progression.

Supplementary Material

Refer to Web version on PubMed Central for supplementary material.

Acknowledgments

We thank Thomas Clements and Lin Zhou for their help and support with experiments and ideas in these studies. We also would like to thank Dr. Daniel A. Harrington for his many helpful insights and reviews, and all members of the Farach-Carson and Carson labs for their continued support. Additionally, we thank Dr. Valera Vasioukhin and her lab at Fred Hutchison Cancer Center for generously providing the hepsin enzyme. Funding for this study was provided by NIH/NCI P01 CA098912 (MCFC and LWC). Additional funding was provided by the Rice University Biochemistry and Cell Biology Department Graduate Student Travel Award.

References

Amalinei C, Caruntu ID, Balan RA. Biology of metalloproteinases. Rom J Morphol Embryol. 2007; 48:323–334. [PubMed: 18060181]

Balasubramani M, Bier ME, Hummel S, Schneider WJ, Halfter W. Perlecan and its immunoglobulin like domain IV are abundant in vitreous and serum of the chick embryo. Matrix Biol. 2004; 23:143–152. [PubMed: 15296942]

Behrens DT, Villone D, Koch M, Brunner G, Sorokin L, Robenek H, Bruckner-Tuderman L, Bruckner P, Hansen U. The epidermal basement membrane is a composite of separate laminin- or collagen IV-containing networks connected by aggregated perlecan, but not by nidogens. J Biol Chem. 2012; 287:18700–18709. [PubMed: 22493504]

Bix G, Fu J, Gonzalez EM, Macro L, Barker A, Campbell S, Zutter MM, Santoro SA, Kim JK, Hook M, Reed CC, Iozzo RV. Endorepellin causes endothelial cell disassembly of actin cytoskeleton and focal adhesions through alpha2beta1 integrin. J Cell Biol. 2004; 166:97–109. [PubMed: 15240572]

Brown AJ, Alicknavitch M, D'Souza SS, Daikoku T, Kirn-Safran CB, Marchetti D, Carson DD, Farach-Carson MC. Heparanase expression and activity influences chondrogenic and osteogenic processes during endochondral bone formation. Bone. 2008; 43:689–699. [PubMed: 18589009]

Cailhier JF, Sirois I, Laplante P, Lepage S, Raymond MA, Brassard N, Prat A, Iozzo RV, Pshezhetsky AV, Hebert MJ. Caspase-3 activation triggers extracellular cathepsin L release and endorepellin proteolysis. J Biol Chem. 2008; 283:27220–27229. [PubMed: 18658137]

Cardillo MR, Di Silverio F, Gentile V. Quantitative immunohistochemical and in situ hybridization analysis of metalloproteinases in prostate cancer. Anticancer Res. 2006; 26:973–982. [PubMed: 16619495]

Chang JH, Javier JA, Chang GY, Oliveira HB, Azar DT. Functional characterization of neostatins, the MMP-derived, enzymatic cleavage products of type XVIII collagen. FEBS Lett. 2005; 579:3601–3606. [PubMed: 15978592]

Christiansen VJ, Jackson KW, Lee KN, McKee PA. Effect of fibroblast activation protein and alpha2-antiplasmin cleaving enzyme on collagen types I, III, and IV. Arch Biochem Biophys. 2007; 457:177–186. [PubMed: 17174263]

d'Ortho MP, Will H, Atkinson S, Butler G, Messent A, Gavrilovic J, Smith B, Timpl R, Zardi L, Murphy G. Membrane-type matrix metalloproteinases 1 and 2 exhibit broad-spectrum proteolytic capacities comparable to many matrix metalloproteinases. Eur J Biochem. 1997; 250:751–757. [PubMed: 9461298]

Datta MW, Hernandez AM, Schlicht MJ, Kahler AJ, DeGueme AM, Dhir R, Shah RB, Farach-Carson C, Barrett A, Datta S. Perlecan, a candidate gene for the CAPB locus, regulates prostate cancer cell growth via the Sonic Hedgehog pathway. Mol Cancer. 2006; 5:9. [PubMed: 16507112]

Farach-Carson MC, Brown AJ, Lynam M, Safran JB, Carson DD. A novel peptide sequence in perlecan domain IV supports cell adhesion, spreading and FAK activation. Matrix Biol. 2008; 27:150–160. [PubMed: 17997086]

Farach-Carson MC, Warren CR, Harrington DA, Carson DD. Border patrol: Insights into the unique role of perlecan/heparan sulfate proteoglycan 2 at cell and tissue borders. Matrix Biol. 2013

Fosang AJ, Neame PJ, Last K, Hardingham TE, Murphy G, Hamilton JA. The interglobular domain of cartilage aggrecan is cleaved by PUMP, gelatinases, and cathepsin B. J Biol Chem. 1992; 267:19470–19474. [PubMed: 1326552]

Fu X, Kassim SY, Parks WC, Heinecke JW. Hypochlorous acid oxygenates the cysteine switch domain of pro-matrilysin (MMP-7). A mechanism for matrix metalloproteinase activation and atherosclerotic plaque rupture by myeloperoxidase. J Biol Chem. 2001; 276:41279–41287. [PubMed: 11533038]

Fuki IV, Iozzo RV, Williams KJ. Perlecan heparan sulfate proteoglycan: a novel receptor that mediates a distinct pathway for ligand catabolism. J Biol Chem. 2000; 275:25742–25750. [PubMed: 10818109]

Giannelli G, Falk-Marzillier J, Schiraldi O, Stetler-Stevenson WG, Quaranta V. Induction of cell migration by matrix metalloprotease-2 cleavage of laminin-5. Science. 1997; 277:225–228. [PubMed: 9211848]

Gohring W, Sasaki T, Heldin CH, Timpl R. Mapping of the binding of platelet-derived growth factor to distinct domains of the basement membrane proteins BM-40 and perlecan and distinction from the BM-40 collagen-binding epitope. Eur J Biochem. 1998; 255:60–66. [PubMed: 9692901]

Gonzalez EM, Reed CC, Bix G, Fu J, Zhang Y, Gopalakrishnan B, Greenspan DS, Iozzo RV. BMP-1/Tolloid-like metalloproteases process endorepellin, the angiostatic C-terminal fragment of perlecan. J Biol Chem. 2005; 280:7080–7087. [PubMed: 15591058]

Gurski LA, Jha AK, Zhang C, Jia X, Farach-Carson MC. Hyaluronic acid-based hydrogels as 3D matrices for in vitro evaluation of chemotherapeutic drugs using poorly adherent prostate cancer cells. Biomaterials. 2009; 30:6076–6085. [PubMed: 19695694]

Hart CA, Scott LJ, Bagley S, Bryden AA, Clarke NW, Lang SH. Role of proteolytic enzymes in human prostate bone metastasis formation: in vivo and in vitro studies. Br J Cancer. 2002; 86:1136–1142. [PubMed: 11953862]

Hashimoto K, Kihira Y, Matuo Y, Usui T. Expression of matrix metalloproteinase-7 and tissue inhibitor of metalloproteinase-1 in human prostate. J Urol. 1998; 160:1872–1876. [PubMed: 9783977]

Heinz A, Jung MC, Duca L, Sippl W, Taddese S, Ihling C, Rusciani A, Jahreis G, Weiss AS, Neubert RH, Schmelzer CE. Degradation of tropoelastin by matrix metalloproteinases–cleavage site specificities and release of matrikines. FEBS J. 2010; 277:1939–1956. [PubMed: 20345904]

Heremans A, van der Schueren B, de Cock B, Paulsson M, Cassiman JJ, van den Berghe H, David G. Matrix-associated heparan sulfate proteoglycan: core protein-specific monoclonal antibodies decorate the pericellular matrix of connective tissue cells and the stromal side of basement membranes. J Cell Biol. 1989; 109:3199–3211. [PubMed: 2687294]

Hopf M, Gohring W, Kohfeldt E, Yamada Y, Timpl R. Recombinant domain IV of perlecan binds to nidogens, laminin-nidogen complex, fibronectin, fibulin-2 and heparin. Eur J Biochem. 1999; 259:917–925. [PubMed: 10092882]

Imai K, Shikata H, Okada Y. Degradation of vitronectin by matrix metalloproteinases-1, -2, -3, -7 and -9. FEBS Lett. 1995; 369:249–251. [PubMed: 7544295]

Iozzo RV. Biosynthesis of heparan sulfate proteoglycan by human colon carcinoma cells and its localization at the cell surface. J Cell Biol. 1984; 99:403–417. [PubMed: 6235235]

Iozzo RV, Zoeller JJ, Nystrom A. Basement membrane proteoglycans: modulators Par Excellence of cancer growth and angiogenesis. Molecules and cells. 2009; 27:503–513. [PubMed: 19466598]

Ishijima M, Suzuki N, Hozumi K, Matsunobu T, Kosaki K, Kaneko H, Hassell JR, Arikawa-Hirasawa E, Yamada Y. Perlecan modulates VEGF signaling and is essential for vascularization in endochondral bone formation. Matrix Biol. 2012; 31:234–245. [PubMed: 22421594]

Jarkovska K, Martinkova J, Liskova L, Halada P, Moos J, Rezabek K, Gadher SJ, Kovarova H. Proteome mining of human follicular fluid reveals a crucial role of complement cascade and key biological pathways in women undergoing in vitro fertilization. J Proteome Res. 2010; 9:1289–1301. [PubMed: 20058866]

Josson S, Matsuoka Y, Chung LW, Zhau HE, Wang R. Tumor-stroma co-evolution in prostate cancer progression and metastasis. Semin Cell Dev Biol. 2010; 21:26–32. [PubMed: 19948237]

Kaneko H, Ishijima M, Futami I, Tomikawa-Ichikawa N, Kosaki K, Sadatsuki R, Yamada Y, Kurosawa H, Kaneko K, Arikawa-Hirasawa E. Synovial perlecan is required for osteophyte formation in knee osteoarthritis. Matrix Biol. 2013; 32:178–187. [PubMed: 23339896]

Kelley LA, Sternberg MJ. Protein structure prediction on the Web: a case study using the Phyre server. Nat Protoc. 2009; 4:363–371. [PubMed: 19247286]

Kelly T, Huang Y, Simms AE, Mazur A. Fibroblast activation protein-alpha: a key modulator of the microenvironment in multiple pathologies. Int Rev Cell Mol Biol. 2012; 297:83–116. [PubMed: 22608558]

Kennett EC, Chuang CY, Degendorfer G, Whitelock JM, Davies MJ. Mechanisms and consequences of oxidative damage to extracellular matrix. Biochem Soc Trans. 2011; 39:1279–1287. [PubMed: 21936802]

Klein G, Conzelmann S, Beck S, Timpl R, Muller CA. Perlecan in human bone marrow: a growth-factor-presenting, but anti-adhesive, extracellular matrix component for hematopoietic cells. Matrix Biol. 1995; 14:457–465. [PubMed: 7795884]

Lamanna WC, Frese MA, Balleininger M, Dierks T. Sulf loss influences N-, 2-O-, and 6-O-sulfation of multiple heparan sulfate proteoglycans and modulates fibroblast growth factor signaling. J Biol Chem. 2008; 283:27724–27735. [PubMed: 18687675]

Lee B, Clarke D, Al Ahmad A, Kahle M, Parham C, Auckland L, Shaw C, Fidanboylu M, Orr AW, Ogunshola O, Fertala A, Thomas SA, Bix GJ. Perlecan domain V is neuroprotective and proangiogenic following ischemic stroke in rodents. The Journal of clinical investigation. 2011; 121:3005–3023. [PubMed: 21747167]

Lynch CC, Hikosaka A, Acuff HB, Martin MD, Kawai N, Singh RK, Vargo-Gogola TC, Begtrup JL, Peterson TE, Fingleton B, Shirai T, Matrisian LM, Futakuchi M. MMP-7 promotes prostate cancer-induced osteolysis via the solubilization of RANKL. Cancer Cell. 2005; 7:485–496. [PubMed: 15894268]

Mongiat M, Sweeney SM, San Antonio JD, Fu J, Iozzo RV. Endorepellin, a novel inhibitor of angiogenesis derived from the C terminus of perlecan. J Biol Chem. 2003; 278:4238–4249. [PubMed: 12435733]

Oda O, Shinzato T, Ohbayashi K, Takai I, Kunimatsu M, Maeda K, Yamanaka N. Purification and characterization of perlecan fragment in urine of end-stage renal failure patients. Clin Chim Acta. 1996; 255:119–132. [PubMed: 8937755]

Pajouh MS, Nagle RB, Breathnach R, Finch JS, Brawer MK, Bowden GT. Expression of metalloproteinase genes in human prostate cancer. J Cancer Res Clin Oncol. 1991; 117:144–150. [PubMed: 1848860]

Perkins DN, Pappin DJ, Creasy DM, Cottrell JS. Probability-based protein identification by searching sequence databases using mass spectrometry data. Electrophoresis. 1999; 20:3551–3567. [PubMed: 10612281]

Platz EA, De Marzo AM. Epidemiology of inflammation and prostate cancer. J Urol. 2004; 171:S36–40. [PubMed: 14713751]

Polyak K, Weinberg RA. Transitions between epithelial and mesenchymal states: acquisition of malignant and stem cell traits. Nat Rev Cancer. 2009; 9:265–273. [PubMed: 19262571]

Powell WC, Knox JD, Navre M, Grogan TM, Kittelson J, Nagle RB, Bowden GT. Expression of the metalloproteinase matrilysin in DU-145 cells increases their invasive potential in severe combined immunodeficient mice. Cancer Res. 1993; 53:417–422. [PubMed: 8417833]

Ra HJ, Harju-Baker S, Zhang F, Linhardt RJ, Wilson CL, Parks WC. Control of promatrilysin (MMP7) activation and substrate-specific activity by sulfated glycosaminoglycans. J Biol Chem. 2009; 284:27924–27932. [PubMed: 19654318]

Reiland J, Sanderson RD, Waguespack M, Barker SA, Long R, Carson DD, Marchetti D. Heparanase degrades syndecan-1 and perlecan heparan sulfate: functional implications for tumor cell invasion. J Biol Chem. 2004; 279:8047–8055. [PubMed: 14630925]

Ritchey ER, Code K, Zelinka CP, Scott MA, Fischer AJ. The chicken cornea as a model of wound healing and neuronal re-innervation. Mol Vis. 2011; 17:2440–2454. [PubMed: 21976955]

Rowe RG, Weiss SJ. Breaching the basement membrane: who, when and how? Trends Cell Biol. 2008; 18:560–574. [PubMed: 18848450]

Strohalm M, Hassman M, Kosata B, Kodicek M. mMass data miner: an open source alternative for mass spectrometric data analysis. Rapid Commun Mass Spectrom. 2008; 22:905–908. [PubMed: 18293430]

Strohalm M, Kavan D, Novak P, Volny M, Havlicek V. mMass 3: a cross-platform software environment for precise analysis of mass spectrometric data. Anal Chem. 2010; 82:4648–4651. [PubMed: 20465224]

Thalmann GN, Sikes RA, Wu TT, Degeorges A, Chang SM, Ozen M, Pathak S, Chung LW. LNCaP progression model of human prostate cancer: androgen-independence and osseous metastasis. Prostate. 2000 Jul.44:91–103. 101;144(102). [PubMed: 10881018]

Tilakaratne WM, Kobayashi T, Ida-Yonemochi H, Swelam W, Yamazaki M, Mikami T, Alvarado CG, Shahidul AM, Maruyama S, Cheng J, Saku T. Matrix metalloproteinase 7 and perlecan in oral epithelial dysplasia and carcinoma in situ: an aid for histopathologic recognition of their cell proliferation centers. J Oral Pathol Med. 2009; 38:348–355. [PubMed: 19239574]

Tripathi M, Nandana S, Yamashita H, Ganesan R, Kirchhofer D, Quaranta V. Laminin-332 is a substrate for hepsin, a protease associated with prostate cancer progression. J Biol Chem. 2008; 283:30576–30584. [PubMed: 18784072]

Turk BE, Huang LL, Piro ET, Cantley LC. Determination of protease cleavage site motifs using mixture-based oriented peptide libraries. Nat Biotechnol. 2001; 19:661–667. [PubMed: 11433279]

Tuxhorn JA, Ayala GE, Smith MJ, Smith VC, Dang TD, Rowley DR. Reactive stroma in human prostate cancer: induction of myofibroblast phenotype and extracellular matrix remodeling. Clin Cancer Res. 2002; 8:2912–2923. [PubMed: 12231536]

Verspurten J, Gevaert K, Declercq W, Vandenabeele P. SitePredicting the cleavage of proteinase substrates. Trends Biochem Sci. 2009; 34:319–323. [PubMed: 19546006]

Vuadens F, Benay C, Crettaz D, Gallot D, Sapin V, Schneider P, Bienvenut WV, Lemery D, Quadroni M, Dastugue B, Tissot JD. Identification of biologic markers of the premature rupture of fetal membranes: proteomic approach. Proteomics. 2003; 3:1521–1525. [PubMed: 12923777]

Warren CR, Grindel BJ, Farach-Carson MC, Carson D. Perlecan/HSPG2 increases in the desmoplastic prostate tumor microenvironment involve transcriptional activation by nuclear factor kappa B. Clinical and Experimental Metastasis. 2013

Webber MM, Waghray A, Bello D. Prostate-specific antigen, a serine protease, facilitates human prostate cancer cell invasion. Clin Cancer Res. 1995; 1:1089–1094. [PubMed: 9815898]

Welch AR, Holman CM, Huber M, Brenner MC, Browner MF, Van Wart HE. Understanding the P1' specificity of the matrix metalloproteinases: effect of S1' pocket mutations in matrilysin and stromelysin-1. Biochemistry. 1996; 35:10103–10109. [PubMed: 8756473]

Whitelock JM, Melrose J, Iozzo RV. Diverse cell signaling events modulated by perlecan. Biochemistry. 2008; 47:11174–11183. [PubMed: 18826258]

Whitelock JM, Murdoch AD, Iozzo RV, Underwood PA. The degradation of human endothelial cell-derived perlecan and release of bound basic fibroblast growth factor by stromelysin, collagenase, plasmin, and heparanases. J Biol Chem. 1996; 271:10079–10086. [PubMed: 8626565]

Woessner JF Jr, Taplin CJ. Purification and properties of a small latent matrix metalloproteinase of the rat uterus. J Biol Chem. 1988; 263:16918–16925. [PubMed: 3182822]

Wu HC, Hsieh JT, Gleave ME, Brown NM, Pathak S, Chung LW. Derivation of androgen-independent human LNCaP prostatic cancer cell sublines: role of bone stromal cells. Int J Cancer. 1994; 57:406–412. [PubMed: 8169003]

Yu WH, Woessner JF Jr. Heparan sulfate proteoglycans as extracellular docking molecules for matrilysin (matrix metalloproteinase 7). J Biol Chem. 2000; 275:4183–4191. [PubMed: 10660581]

Zhang Z, Marshall AG. A universal algorithm for fast and automated charge state deconvolution of electrospray mass-to-charge ratio spectra. J Am Soc Mass Spectrom. 1998; 9:225–233. [PubMed: 9879360]

Highlights

- Glycosylated and basement membrane bound perlecan is cleaved by MMP-7.
- MMP-7 cleavage of perlecan produces large domain IV fragments.
- MMP-7 degrades the basement membrane to allow prostate cancer cell invasion.
- Perlecan domain IV induces clustering in metastatic prostate cancer cells.
- MMP-7 proteolysis of domain IV reverses clustering in favor of cell dispersion.

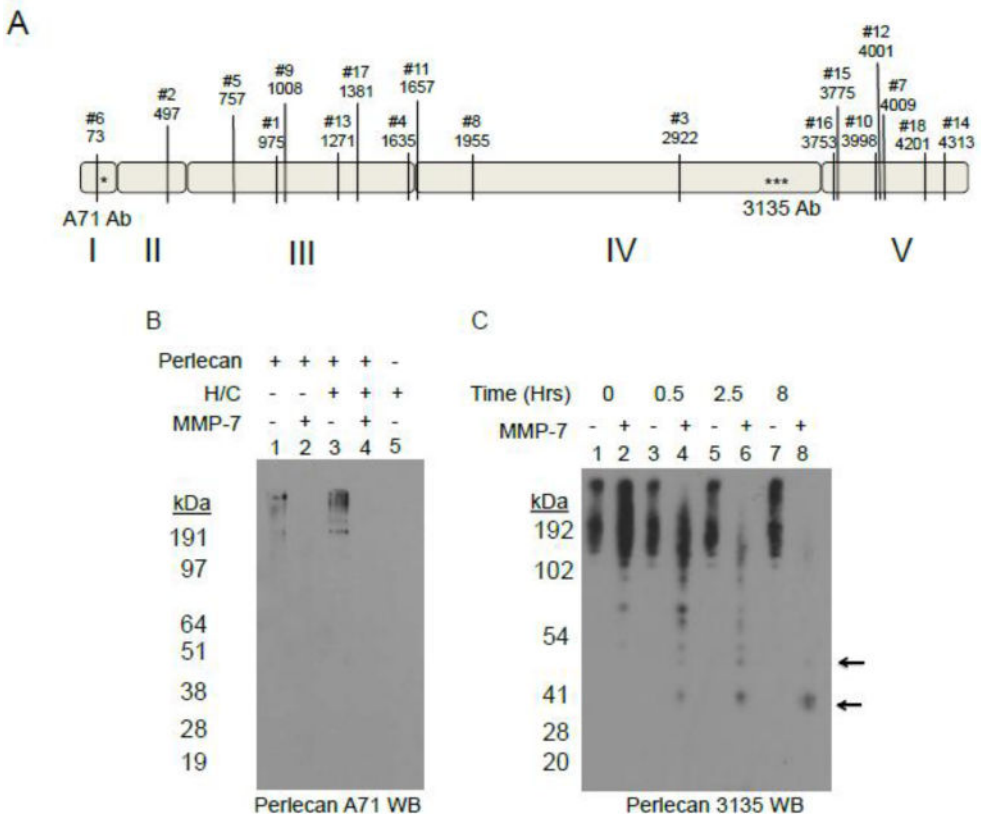

Figure 1. MMP-7 cleavage of full length perlecan *in silico* and *in vitro.*

A) Perlecan sequence (UniProt: P98160) was queried against MMP-7 proteolytic sites with online Site Prediction software under default conditions (http://www.dmbr.ugent.be/prx/bioit2-public/SitePrediction/index.php). Shown are the top ranked 18 positions by Average Score not including the signal sequence. All have specificities greater than 99% with a majority of the predicted sites occurring in domain III and domain V. The asterisks indicate the approximate epitope site of the A71 monoclonal antibody (in domain I) and 3135 polyclonal antibody (in domain IV). B) Western blot (A71) of WiDr purified perlecan either pre-treated or not with combination of heparitinases I, II, III and chondroitinase ABC (H/C) and then incubated with or without MMP-7 (2.5 hr at 37°C 4 μg perlecan, 0.4 μg MMP-7). Lane 1: Control perlecan incubation with no enzyme; Lane 2: perlecan with MMP-7; Lane 3: perlecan pre-treated with H/C; Lane 4: perlecan pretreated with H/C and incubated with MMP-7; Lane 5: H/C combination control. C) Western blot (3135) of an 8 hr time course digestion of perlecan with or without MMP-7. The arrows indicate discrete fragments of approximately 50 kD and 35 kD after incubation with MMP-7, but absent without.

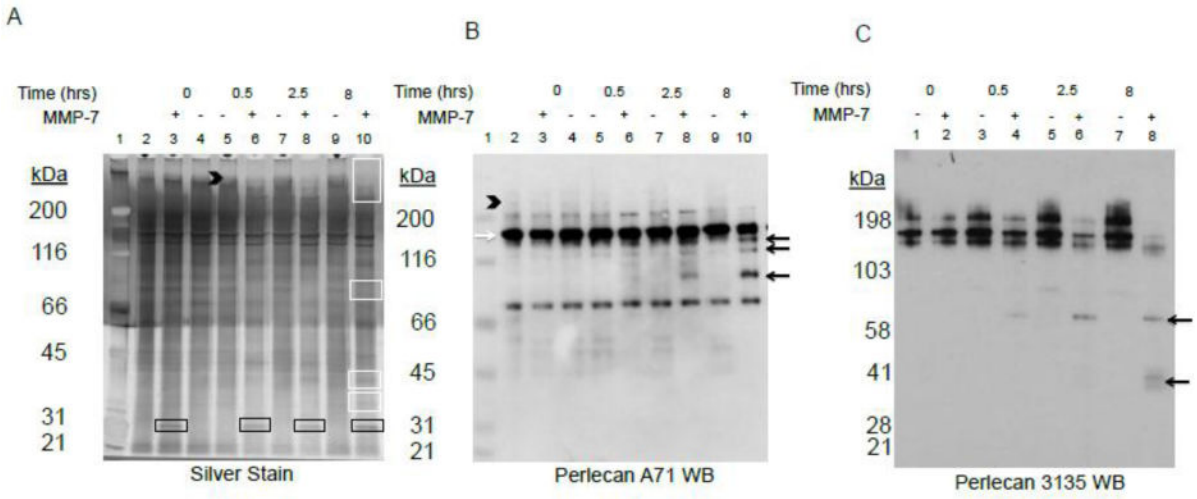

Figure 2. MMP-7 time course digestion of placental human basement membrane (BM) extract

Polymerized BM extract was incubated with or without MMP-7 for various time points up to 8 hrs and subjected to A) silver stain, B) antibody A71 western blot, or C) antibody 3135 western blot. The first lane in A and B is the MW standard marker and the second lane contains control BM never polymerized. The black arrowhead indicates high molecular weight glycosylated protein. The white boxes in panel A highlight bands created or destroyed with MMP-7 digestion. The black boxes indicate the primary MMP-7 band, not digestion products. The white arrow is the primary A71 and 3135 positive perlecan band and the black arrows highlight the bands generated during MMP-7 incubation.

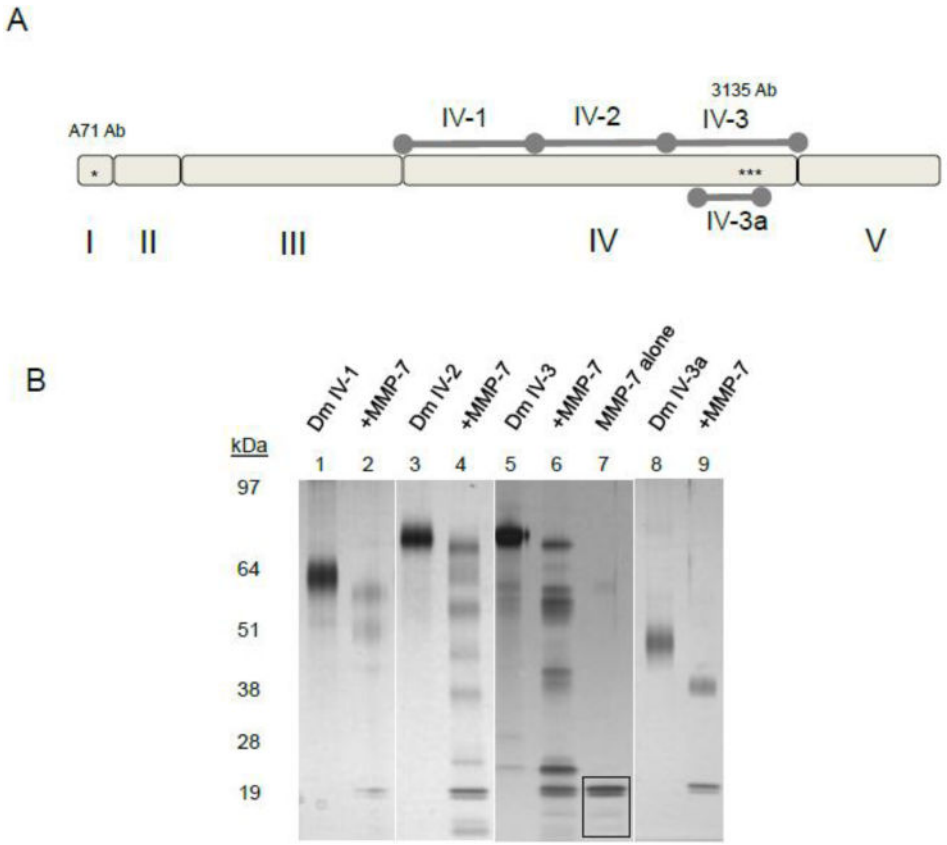

Figure 3. Recombinant perlecan Dm IV cleavage by MMP-7

A) Diagram of recombinant subdomains Dm IV-1, 2, 3, and Dm 3a compared to full length perlecan. B.) Digestion of recombinant domain IV protein by MMP-7. Various subdomains of Dm IV: IV-1 (lanes 1,2), Dm IV-2 (lanes 3, 4), Dm IV-3 (lanes 5, 6), Dm IV-3a (lanes 8,9) were incubated alone or with MMP-7 (1 μg of Dm IV with 0.1 μg MMP-7) overnight at 37°C. Shown is a silver stain after SDS-PAGE separation on a 4–12% (w/v) acrylamide gradient gel. MMP-7 can cleave every subdomain. The black boxed portion in lane 7 (MMP-7 alone) indicates the MMP-7 band.

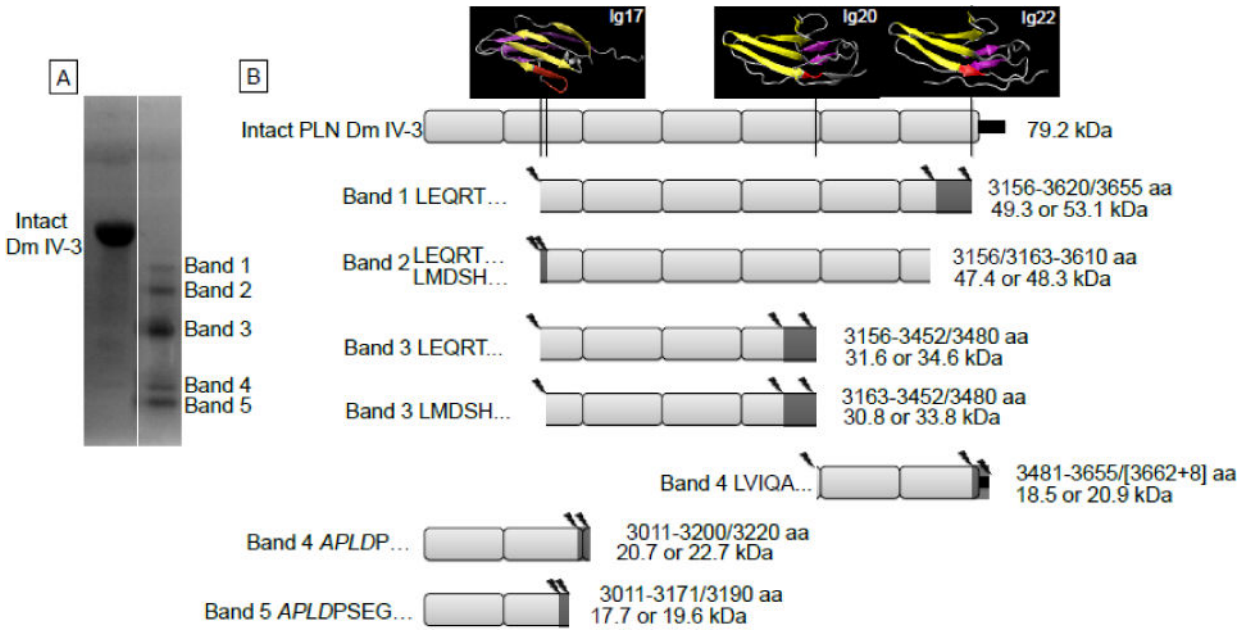

Figure 4. Perlecan Dm IV-3 cleavage patterns by MMP-7

A) The Coomassie stained PVDF membrane of Dm IV-3 either alone (intact) or incubated with MMP-7. The five primary protein bands were analyzed for N-terminal sequencing by Edman degradation. B) Likely cleavage patterns for each band of MMP-7 digested Dm IV-3 given the sequenced N-termini, MALDI mass measurements and LC-MS/MS identified peptides. The left side of each indicated fragment identifies the band N-terminus sequencing found, and the right indicates the likely C-terminus amino acids (amino acid, aa) MMP-7 cleavage site and the resultant apparent molecular weight (kDa) that corresponds approximately to the masses found by MALDI and in the Coomassie stained PVDF. Above intact Dm IV-3 are the PHYRE modeled Ig modules with the indicated MMP-7 cleavage sites shown in red. Cleavage mostly occurs at amino acids in the linking region between Ig modules or in the middle of the Ig module linking the interfacing beta strands. Additionally, each MMP-7 cleavage site produces an aliphatic N-terminus such as leucine, isoleucine, or valine. The small black rectangle at the end of the Dm IV-3 schematic indicates the V5 epitope and polyhistidine tag. The asterisks indicate the 3135 polyclonal antibody binding site on Dm IV-3.

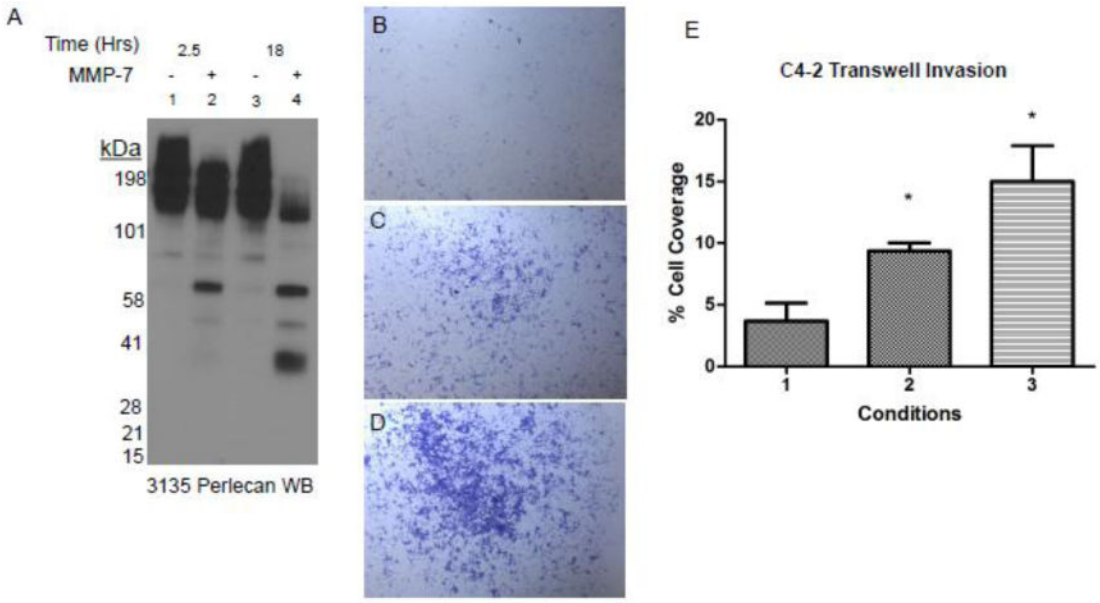

Figure 5. Transwell® invasion assay of C4-2 PCa cells through a basement membrane (BM) extract

A) BM extract was incubated in serum free medium either with or without MMP-7 over 18 hrs to replicate the conditions in the Transwell® invasion assay. A western blot using 3135 antibody reveals the same fragmentation pattern as does digestion in the presence of detergents. Images of crystal violet stained C4-2 cells that have entered the Transwell® membrane through (B) BM extract alone, (C) BM extract pre-digested with MMP-7, or (D) BM extract coated and then digested on the plate with MMP-7. E) Quantification of invasion assay on various conditions: 1) BM extract alone; 2) BM extract pre-digested with MMP-7; 3) BM extract coated and then digested with MMP-7. Unpaired student's t-test comparing to condition 1; *= p value <0.05.

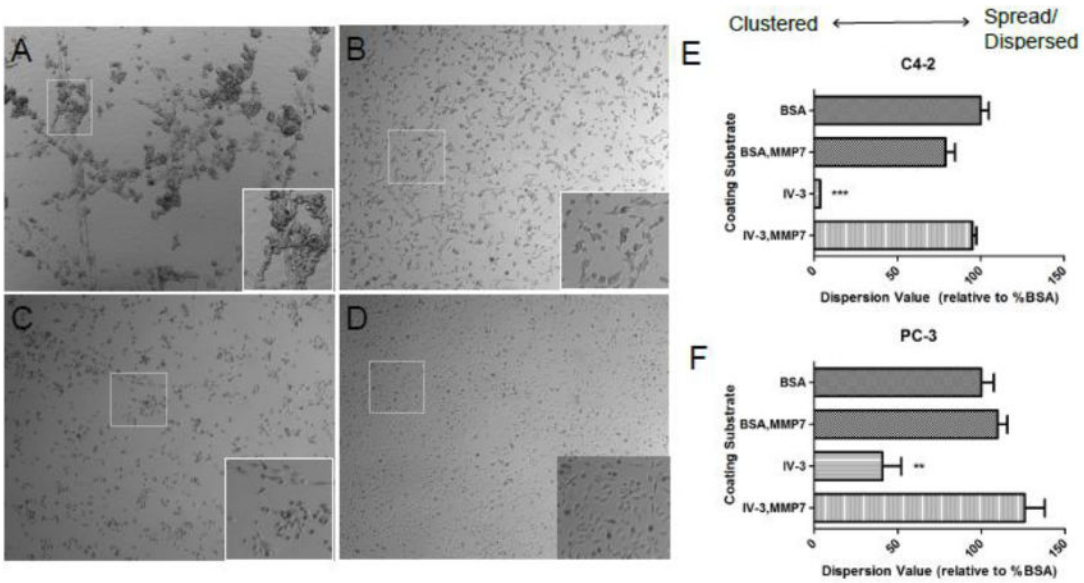

Figure 6. Cell clustering induced by perlecan Dm IV-3 and reversed by MMP-7

C4-2 (A, B) and PC-3 PCa cells (C, D) seeded on adsorbed Dm IV-3 (A, C) or Dm IV-3 pre-digested with MMP-7 (B, D). Cell clustering occurred for both cell types on Dm IV-3 but was reversed with MMP-7 digestion. Quantification of cell dispersion is shown for C4-2 (E) and PC-3 (F) cells on various matrix types. A lower value is indicative of cell clustering. A *** indicates a p value <0.005 and ** is a p value <0.01 in comparison to Dm IV-3 + MMP-7 using an unpaired student's t-test.

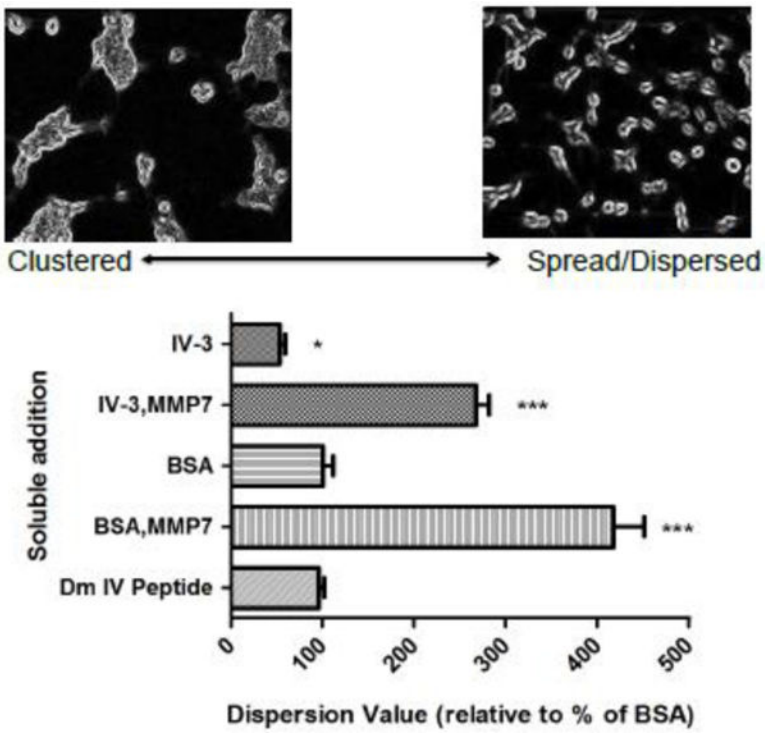

Figure 7. Soluble digest mixtures and peptide effect on dispersion/spreading of C4-2 cells introduced to a Dm IV-3 substrate

Dm IV-3 was adsorbed to wells and seeded simultaneously with C4-2 cells with the following overnight digests in soluble form: IV-3 alone, IV-3 incubated with MMP-7, BSA alone, BSA incubated with MMP-7, and 20 μg/mL Dm IV peptide. The lower the value the more clustered (left representative image) and the higher the value the more dispersed/spread (right representative image) and are presented in % relation to control BSA addition. Significance values are in relation to control BSA soluble addition; * $p < 0.05$, *** $p < 0.001$.